Possible climatic controls on the accumulation of Peru's most prominent alluvial fan: The Lima Conglomerate

Camille Litty[1,3], Fritz Schlunegger[1], Naki Akçar[1], Pierre Lanari[1], Marcus Christl[2], Christof Vockenhuber[2]

[1] *Institute of Geological Sciences, University of Bern, Baltzerstrasse 1+3, CH- 3012 Bern.*

[2] *Laboratory of Ion Beam Physics, ETH Zurich, Zurich, Switzerland.*

[3] *Current address : Université de Lorraine, Centre de recherches pétrographiques et géochimiques, Nancy, France*

ABSTRACT

Sediment accumulation can occur in response to a change in either tectonic or climatic driving forces. Here, we explore these controls on the deposition of the Lima Conglomerate, Peru. We use a combination of quantitative methods to explore the age of sediment accumulation, the provenance of the material and the paleo-erosion rates recorded by these deposits. Isochron burial dating with cosmogenic ^{10}Be and ^{26}Al yield an age of c. 500 ka for the base (490 ± 70 ka) and the uppermost sample situated c. 30 m higher upsection (490 ± 80 ka). Results of paleo-erosion rate estimates with concentrations of in-situ ^{10}Be show a c. 60% increase from 105 ± 10 mm ka^{-1} for the base to 169 ± 14 mm ka^{-1} for the uppermost sample. Finally, provenance tracing with in-situ U/Pb ages on detrital zircon implies that the material has been derived from the entire drainage basin. The combination of results suggests that sediment accumulation occurred in response to an erosional pulse, which affected the entire basin within a short time interval. Because ^{10}Be data represents a large spatial record of erosion, we exclude the possibility where a breakout of a lake or a focused release of material in response to earthquakes, were responsible for the large material flux. Instead, the erosional pulse was likely to have occurred at the scale of the entire basin, supporting the idea of a larger-scale,

This article has been accepted for publication and undergone full peer review but has not been through the copyediting, typesetting, pagination and proofreading process which may lead to differences between this version and the Version of Record. Please cite this article as doi: 10.1002/esp.4548

most likely climate driven control. In this context, the accumulation age of c. 500 ka falls into an orbital cycle fostering the emerging picture in the literature that sediment routing in the Andes have most likely been driven by climate and cyclic changes. We suggest that the Andean mountain range offers an ideal laboratory to explore the erosional history in relation to climate patterns, at least in Peru.

Keywords: Lima Conglomerate; cosmogenic nuclides; isochron burial dating, paleo erosion rates, U-Pb in-situ zircon dating, sediment provenance

INTRODUCTION

Terrace deposits with material sources in mountain belts represent important archives of past environmental and tectonic changes. These sediments can record modifications in paleo-water discharge, which is a proxy for precipitation rates and climate (Sylvia and Galloway, 2006; D'Arcy et al., 2017; Litty et al., 2017). They can also record the response to earthquake induced landslides (Dadson et al., 2003; McPhillips et al., 2014), and changes in tectonic uplift rates. The reconstruction of the timing and the rate of alluvial sediment deposition, paired with information about the provenance of the material bear important information when the scope lies in the detection of specific climate or seismic events as driving forces on erosion and sediment fluxes. This has particularly been the case for the Central Andes (Strecker et al., 2007), where previous studies have identified a strong environmental control on erosion (Reber et al., 2017), sediment transfer, landscape form (Montgomery et al., 2001; Trauerstein et al., 2013) and the construction of terrace sequences particularly in the Andes (Steffen et al., 2009; Bekaddour et al., 2014; Savi et al., 2016; Tofelde et al., 2017). In this context, it has been proposed that variations in precipitation rates and patterns have led to remarkable lake-level variations on the Altiplano (Fritz et al., 2004). These climate changes, with orbital frequencies of c. 100 ka, 40 ka and 20 ka, were also considered to have controlled pulses of erosion and sediment discharge by modulating the fluvial runoff on the western Andean margin (e.g.,

Steffen et al., 2009; Bekaddour et al., 2014; Veit et al., 2016; Litty et al., 2017), which in turn, has been interpreted as being the main factor controlling the formation of cut-and-fill terrace systems in this region (Norton et al., 2016). Accordingly, the Andean mountain range could be perceived as an ideal laboratory for exploring a climate forcing not only on surface mass fluxes, but also on the tectonic history of this mountain belt through a positive feedback to climate change (Norton and Schlunegger, 2011). However, the interpretation of climate, and more specifically of an orbital control on surface mass flux and the construction of terrace sequences is based on three archives only that are sparkled along the Peruvian coast over a distance of c. 1000 km: Pativilca at 10°42'S (Trauerstein et al., 2014; Litty et al., 2018); the Pisco valley at 13°42'S (Steffen et al., 2009) and the Majes valley at 16°13'S latitudes (Steffen et al., 2010). We complement this dataset through the analysis of the fan deposits, situated Lima at 12°03'S.

In this paper, we explore the hypothesis whether the construction of terrace deposits along the Peruvian coastal margin records a possible orbital control on the erosional history of the adjacent Andean mountain belt. We complement an already existing database and focus on the terrace deposits at Lima, where we explore the geological history of these deposits and underlying controls with dating and provenance tracing techniques, and through the estimation of paleo-denudation rates. As a first effort, we date the deposits using isochron burial dating technologies thereby using in-situ cosmogenic ^{10}Be and ^{26}Al. We use these age constraints to explore possible correlations with any known period of enhanced precipitation, interglacial stades or tectonic activity in an effort to distinguish between the different possible controlling mechanisms leading to sediment accumulation. Second, the paleo-basin wide denudation rates, recorded at different levels of the sedimentary sequence, will be determined using concentrations of in-situ cosmogenic ^{10}Be preserved in these sediments. This will allow us to determine if the sediment accumulation period also records a pulse of erosion. Finally, we will determine the provenance of the fine-grained sediments embedded in the conglomerate through detrital zircon U/Pb in-situ dating techniques, which will constrain the location where the erosion of the Lima Conglomerate material occurred. These new information will support the emerging picture of an orbital control on erosion, sediment transport and the construction of terraces in the Andes.

REGIONAL SETTING

Chronology and sedimentology of the Lima Conglomerate

The Lima Conglomerate (Figure 1 and 2; Karakouzian et al., 1996) is an alluvial fan made up of coarse-grained massive-bedded conglomerates with minor interbedded sandstones and mudstones. The best exposures can been found along the Pacific coast near Miraflores, a southern district of the city of Lima. There, this unit is made up of an up to 80 m-thick stack of poorly sorted, clast-supported conglomerates with a coarse-grained sandy matrix. The fan stretches along the Pacific coast over a distance of 15 km, and it has a convex-up, fan-shaped asymmetric geometry (Figure 1). This suggests that the Lima Conglomerate forms one single fan. The sediments were deposited by the Chillon and Rimac Rivers that have their origins in the Andes c. 120 km farther upstream at an elevation of c. 4800 m a.s.l. (Figure 1).

Karakouzian et al. (1996) suggested a Pleistocene age for these deposits, without providing constraints on their age assignment. Le Roux et al. (2000) proposed a middle Pleistocene age on the grounds of geomorphologic, stratigraphic and soil-stratigraphic evidence. The only fossiliferous evidence to infer an age, at least to our knowledge, is from the top of this formation, where a molar tooth of Equus curvidens Owen, which is of Pleistocene age, was recovered (Lisson, 1907). However, in spite of good outcrops along the coast no results of any dating campaigns have ever been published. This paper thus reports the first numerical age of the Lima Conglomerate deposits and aims at unravelling the controls on the deposition of the fan delta.

The clasts embedded within the conglomerates are subrounded and sometimes imbricated, but the sedimentary fabrics are predominantly massive. The contact between the conglomerate suite and the underlying basement is situated below sea level and cannot be constrained. The sedimentological architecture of the exposed succession is characterized by an amalgamation of several meter-thick units. Each of them has an erosive basal contact indicating deposition after rapid channel flow, as noted by Le Roux et al. (2000). The same authors found that cross-beds with meter-high shallow-dipping foresets, or alternatively troughs with several meters-wide diameters, alternate with massive-bedded structures that appear as the dominant facies. Sandstones within the conglomerate are mostly

lenticular, overlying erosional surfaces. Most of the sandstones are trough cross-laminated, although antidune cross-lamination and low-angle tabular cross-lamination were also observed (Le Roux et al., 2000). Sandstone beds or lenses commonly fine upward into siltstone and mudstone, suggesting waning currents after high-discharge episodes (Le Roux et al., 2000). These facies-associations suggest the supply, transport and deposition of coarse-grained bedload by braided streams (Miall, 1985) that formed an alluvial fan where the frontal part has now been eroded subsequent to deposition. In these environments where braiding occurs, cross-bedded conglomerates on top of an erosive base point to the occurrence of gravelly bedforms in shallow channels, while massive-bedded conglomerates with sandstone lenses were most likely formed on top of longitudinal bars, where sand becomes deposited during waning floods in a high energy environment of rapidly shifting braided channels (Miall, 1985; Le Roux et al., 2000). There is a complete absence of any signs of marine influence (e.g. beach imbrication, and marine fossils) in the exposed part of the succession, which suggests that the conglomerates have not been reworked by waves (Le Roux et al., 2000). Mapping in the field discloses a lens-shaped cross-sectional geometry for the top surface of the Lima Conglomerate, which stretches over a distance of > 15 km parallel to the Pacific coast (Figure 1). The surface of the Lima unit thus displays all characteristics of an alluvial fan: it is situated next to an ocean, the surface is convex-up in a section perpendicular to the flow and the surface is highest along the fan axis (Figure 1).

Bedrock geology of the source area

The clasts encountered in the Lima Conglomerate reflect the composition of the Andean Cordillera and mainly comprise diorites, granodiorites, granites and gabbros derived from the Late Cretaceous Coastal Batholith. Mesozoic and Cenozoic volcanic as well as pyroclastic constituents also occur in the clast suite of the conglomerate (LeRoux et al., 2000; Figure 1). In the area surrounding the Lima drainage basin, the chronology of the intrusion of the batholith was established in detail by Wilson (1975), who identified three intrusive episodes separated by periods of relative magmatic quiescence. These include: The emplacement of the gabbroic, meladioritic, and tonalitic

plutons c. 105-85 Ma ago; the intrusion of the granodioritic plutons c. 75-56 Ma ago; and the formation of the granites and monzogranites c. 39-35 Ma ago.

Climate

The precipitation pattern of the western Peruvian Andes is strongly influenced by the Andean mountain range, which acts as a major topographic barrier to the atmospheric circulation. The precipitation pattern is also related to the position of the Intertropical Convergence Zone (ITCZ) associated with orographic effects on the eastern side of the Andes (Bookhagen and Strecker, 2008). The climate is characterized by wet phases and strong precipitation rates during austral summer, particularly on the Altiplano, and by dry persistent westerly winds with almost no precipitation during austral winter. During this period, the western side of the Peruvian Andes experiences zero precipitation. As a result, precipitation rates in the Rio Rimac and Chillon basins decrease from East to West, with an annual precipitation rate up to 400 mm on the Altiplano down to c. 0 mm per year in the coastal area.

On orbital time scales, the position of the ITCZ has shifted in response to larger heat contrasts between the Northern and Southern Hemispheres, which has been related to the effects of shifts in the Earth's orbital parameters (Strecker et al., 2007). The results are stronger upper air easterlies and more precipitation on the Altiplano during time intervals of larger insolation on the Altiplano (Garreaud et al., 2003; Strecker et al., 2007). Variations in precipitation rates and patterns led to remarkable lake-level variations on the Altiplano as recorded by lake levels highstands on the plateau (Fritz et al., 2004). These shifts in precipitation rates were also considered to have resulted in changes in the loci of erosion as provenance tracing techniques have shown (Litty et al., 2017), and in changes in erosion rates as suggested by concentrations of in-situ ^{10}Be measured in terrace material along the Pisco valley (Bekaddour et al., 2014).

SAMPLING SITES

Three levels, on a vertical transect, on the coastal cliff of the Lima Conglomerate in the district of Miraflores, have been sampled for $^{10}Be/^{26}Al$ isochron burial dating, paleo-erosion rates and provenance tracing purposes (Figure 2; Table 1). This transect has been selected because of its accessibility thanks to the presence of stairs from the bottom of the cliff to the top in Miraflores (Figure 2B). In particular, we collected samples from three levels including site LIM-IS3, which is the lowermost level of the deposits (Figure 2C and 2D), site LIM-IS2 representing an intermediate level (24 m above site LIM-IS3; Figure 2E and 2F) and site LIM-IS1 corresponding to the topmost level of the sequence (33 m above site LIM-IS3; Figure 2G and 2H). At LIM-IS3, three quartz bearing pebbles have been collected, while six quartz bearing clasts were taken at site LIM-IS2 and four quartz rich pebbles have been used for the measurement of the isochron at LIM-IS1. In addition, three sand samples, one at each level (sand samples LIM-PE3, LIM-PE2 and LIM-PE1 form base to top), have been collected from the matrix of the conglomerates for the calculations of the paleo-basin wide denudation rates. Finally, the same sand samples have been used to infer the provenance of the fine-grained sediments.

METHODS

Isochron burial dating

Over the past 25 years, cosmogenic nuclides have become an essential tool in Quaternary geochronology (Granger, 2006; Gosse and Phillips, 2001; Schaller et al., 2016). The cosmogenic ^{26}Al-^{10}Be isochron burial dating method (Balco and Rovey, 2008; Erlanger et al., 2012; Akçar et al., 2017) has been employed to determine burial ages and to establish the timing of deposition of the alluvial material. This dating technique is based on the difference in half-lives of ^{10}Be (1.387 Ma; Korschinek et al., 2010 and Chmeleff et al., 2010) and ^{26}Al (0.705 Ma; Norris et al., 1983). We collected samples from the same stratigraphic level, thereby assuming that they were deposited at nearly the same time. No tectonic offsets are found in the field, which suggests that the deposits have not been deformed or faulted since the time of their deposition. Accordingly, a horizontal line represents a same

stratigraphic level. This method works if the collected material has different inherited nuclide concentrations but the same post-burial production history (Balco and Rovey, 2008, Darling et al., 2012, Erlanger et al., 2012, Balco et al., 2013 and Çiner et al., 2015; Bender et al., 2016; Akçar et al., 2017). When the measured ^{26}Al concentrations are plotted against ^{10}Be concentrations, they should fall on a line, referred to as the isochron (Balco et al., 2008 and Erlanger et al., 2012). The slope of the regression line is used to determine the ^{26}Al/^{10}Be ratio at the time of burial and thus the depositional age (for further details see Balco and Rovey, 2008, Darling et al., 2012, Erlanger et al., 2012, Balco et al., 2013 and Çiner et al., 2015).

The ^{26}Al-^{10}Be isochron burial method provides several key advantages for dating conglomerate deposits in general and the Lima Conglomerate in particular. First, the isochron burial method works well for sediments that are between ~0.1 and ~5.0 Ma old (Granger, 2006). Given that former studies have suggested a Pleistocene age for this unit (Lisson, 1907; Karakouzian et al., 1996), we expected the age of the accumulation of the Lima Conglomerate material to fall within this range.

The collected samples were processed in the Surface Exposure Laboratory of the Institute of Geological Sciences at the University of Bern following the lab protocol described in Akçar et al. (2012). Cosmogenic ^{10}Be and ^{26}Al were extracted according to Akçar et al. (2012) for accelerator mass spectrometer measurement (AMS) at the ETH Zurich (Christl et al., 2013; Kubik & Christl, 2010). Inductively coupled plasma optical emission spectrometry (ICP-OES) at the Department of Chemistry and Biochemistry of the University of Bern was used to determine the total Al and native ^{9}Be concentrations of the samples. The ^{10}Be/^{9}Be and ^{26}Al/^{27}Al AMS measurements were then performed at the tandem facility at the ETH Zurich (Christl et al., 2013). A long-term weighted average ^{10}Be/^{9}Be ratio of $(2.51 \pm 0.53) \times 10^{-15}$ was used for full process blank correction. To calculate the isochron burial age, a ^{26}Al/^{10}Be surface production ratio of 6.75 has been used. A production rate of cosmogenic ^{10}Be at the surface at sea level-high latitude (SLHL) of 4.00 ± 0.32 atoms $g^{-1}SiO2^{-1}a^{-1}$ has been applied (Borchers et al., 2016). The altitude and latitude scaling of the surface production rate was calculated according to Lal (1991) and Stone (2000). The isochron-burial age was then calculated according to the steps described in detail in Erlanger et al. (2012) using the MATLAB® software package and the script provided by Darryl Granger (personal communication, 2016).

Paleo erosion rates

Paleo-basin wide erosion rates ε can be calculated using the cosmogenic nuclide concentrations of past sediment samples N_0 following Granger et al. (1996), where:

$$N_0 = \frac{P_0}{\lambda + \frac{\rho\varepsilon}{\Lambda}}\left(1 - e^{-\left(\lambda + \frac{\rho\varepsilon}{\Lambda}\right)t}\right) \quad (1).$$

Here, P_0 is the nuclide production rate of a particular nuclide at the surface (atoms $g^{-1}.a^{-1}$), t is the time since deposition (year), ρ is the bulk density of the sedimentary material ($g.cm^{-3}$), λ is the radioactive decay constant of a nuclide (a^{-1}) and Λ is the attenuation length ($g\ cm^{-2}$).

The equation (eq. 1) is used to calculate a basin wide paleo-erosion rate based on cosmogenic nuclide concentrations of the sand embedded in the Lima Conglomerate deposits after corrections have been made for: post depositional nuclide production at sample depth z and atom loss due to radioactive decay during time t (both considered in eq. 1). These equations can be used assuming: (i) The material was well mixed in the upstream basin and finally embedded in the terrace fill. This appears to be the case in the western Peruvian valleys where the fluvial processes have dominated the transport of sediment (Litty et al., 2017), thus providing well-mixed material. (ii) The paleo-erosion is representative for the entire catchment. Indeed, the sediments of the Pleistocene terrace fills in western Peru record an origin from both the upper flat part of the catchments and the lower steep reaches (Litty et al., 2017). (iii) The residence of the material on the hillslopes and the channels is much shorter than the erosional timescale. This is the case in the western Peruvian valleys where regolith was considered to have been rapidly stripped from hillslopes, which most likely resulted in the supply of large volumes of sediment to the trunk streams during the periods of sediment aggradation (Norton et al., 2016). (v) The individual sedimentary sequences have not experienced multiple phases of erosion and re-deposition, so major internal unconformities are not present (von Blanckenburg, 2005). This appears to be the case in the sampled vertical transect as no unconformities in the conglomerate sequence have been observed in the field. This inference will also be confirmed

by the age results. Calculations were accomplished using the default parameters in CAIRN, that include a ^{10}Be half-life of 1.39 ± 0.01 Ma (Chmeleff et al., 2010; Korschinek et al., 2010) and a SLHL ^{10}Be production rate of 4.00 ± 0.32 at $g^{-1}.a^{-1}$ (Braucher et al., 2011) and that consider the neutron, fast and slow muon attenuation lengths and contribution (Braucher et al., 2011).

Sediment provenance through U/Pb dating of detrital zircon

U–Pb dating of detrital zircons from clastic sediments by LA-ICPMS has become a frequently used method in sedimentary provenance studies (Fedo et al., 2003; Litty et al., 2017). U–Pb in-situ ages on single detrital zircon grains were used to identify the provenance components recorded at the three different levels of the Lima Conglomerate. Samples were crushed and sieved within the 100-400 μm fractions. The zircons were separated using magnetic and heavy liquid techniques. Random handpicked zircons were mounted in epoxy-filled or acrylic grain mount blocks and polished to expose the interior of the grains suitable for ion probe and laser-ablation–inductively coupled plasma–mass spectrometry analysis (LA-ICP-MS). All grains were imaged by a ZEISS EVO 50 Scanning Electron Microscope at the University of Bern in order to investigate their morphology and to collect high-resolution images unravelling the internal microstructures and chemical zoning. The first observations on zircon crystals were realized in VPSE (Variable Pressure Secondary Electrons Detector) mode using 20–10 keV, 100 μA beam current, ~10 mm working distance at ~20–10 Pa chamber pressure, to examine the possible presence of inclusions of other minerals that can influence the U-Pb isotopic results. The most suitable locations of the spots for U-Pb analyses were then selected on the grain rims where neither inclusions nor strong chemical zoning were found. U/Pb measurements were conducted at the Institute of Geological Sciences of the University of Bern using a GeoLas-Pro 193 nm ArF Excimer laser system (Lambda Physik) combined with an Elan quadrupole mass spectrometer. Detailed analytical protocols are reported in Kunz et al. (2017). Ablation was conducted at an energy density of 2.5 J cm^{-2} with a repetition rate of 9 Hz using a spot size of 24 μm. Zircon standard GJ-1 (Jackson et al. 2004), and glass reference material NIST SRM 612 has been

used for the quantification of isotopic and element concentrations. Accuracy and long term reproducibility was monitored using zircon standard Plešovice (337.13 ± 0.37 Ma; Sláma et al. 2008). Data reduction for U/Pb-dating was done using the software Iolite 2.5 (Paton et al. 2010) following Petrus and Kamber (2012). Visual age data reduction schemes and error propagation methods are built into U-Pb Geochronology Iolite Software. Only grains with concordant U-Pb ages have been used.

One of the main problems in detrital zircon geochronology is to determine the minimum number of grains to be analysed to ensure that all populations are detected. In addition, the geological information that can be extracted from a set of age data on detrital zircons is critically dependent on the number of analyzed grains (Vermeesch, 2004). Indeed, a distribution with one single age cluster is unlikely to occur in natural sediments. In a more realistic scenario, sediments may contain several age populations, each of which having a non-uniform age distribution. Previous studies about the provenance of sediments that used U–Pb dating of detrital zircon (Morton et al., 1996) have shown that precise and accurate U–Pb ages of 80 to 100 zircon grains in each sample are needed for a reliable identification of the major sedimentary sources (Dodson et al., 1988). However, Andersen (2005) suggested that the random fraction should comprise 35–70 grains or more, depending on the complexity of the age-pattern of a specific sample. Andersen (2005) suggested that the relative error in the population size decreases with increasing number of analyses, but that this decrease occurs only slowly for small populations. Here, 58 and 63 zircons have been dated for the modern samples LIM-ME and LIM-ME2 respectively and 107, 44 and 70 zircons have been dated for the terrace samples LIM-PE1, LIM-PE2 and LIM-PE3 respectively.

RESULTS

Isochron burial dating

AMS-measured $^{10}Be/^{9}Be$ and $^{26}Al/^{27}Al$ ratios (with uncertainties) as well as calculated ^{10}Be, ^{26}Al concentrations and $^{26}Al/^{10}Be$ ratio for each sample are shown in Table 2. The ^{10}Be concentrations of the four samples of the upper part of the sequence (LIM-IS1) vary from c. 14 x 10^3 atoms g^{-1} (LIM-IS1-4) to 170 x 10^3 atoms g^{-1} (LIM-IS1-1) and the ^{26}Al concentrations from c. 82 x 10^3 atoms g^{-1} to 740 x 10^3 atoms g^{-1} for the same samples, respectively (Table 2). The $^{26}Al/^{10}Be$ ratios vary from 4,37 ± 1,79 (LIM-IS1-1) to 6,74 ± 0,93 (LIM-IS1-8). The ^{10}Be concentrations of the six samples of the middle part of the sequence (LIM-IS2) span the range from c. 10 x 10^3 atoms g^{-1} (LIM-IS2-6) to 37 x 10^3 atoms g^{-1} (LIM-IS2-9) and the ^{26}Al concentrations from c. 7 x 10^3 atoms g^{-1} (LIM-IS2-4) to 445 x 10^3 atoms g^{-1} (LIM-IS2-9). The $^{26}Al/^{10}Be$ ratios range from 8,09 ± 0,87 to 33,5 ± 12. Finally, the ^{10}Be concentrations of the three samples of the bottom part of the sequence (LIM-IS3) vary from c. 13 x 10^3 atoms g^{-1} (LIM-IS3-5) to 121 x 10^3 atoms g^{-1} (LIM-IS3-2) and the ^{26}Al concentrations from c. 107 x 10^3 atoms g^{-1} to 121 x 10^3 atoms g^{-1} for the same samples, respectively. The $^{26}Al/^{10}Be$ ratios range from 5,71 ± 0,19 to 8,18 ± 0,85. The measured ^{26}Al concentrations are plotted versus ^{10}Be concentrations including 1σ uncertainties (Figure 3). The results from the isochron burial dating yield a burial age of c. 500 ka, i.e. 490 ± 70 ka for the bottom part of the sequence and a burial age of 490 ± 80 ka for the top part of the Lima Conglomerate (Figure 4). This represents the first accumulation age of the Lima Conglomerate and the first isochron burial age from alluvial deposits in the Andes. The two isochron burial dating results show an identical age for the top and the bottom levels despite a difference of more than 30 meters of elevation in-between the sampling sites. Unfortunately, it is not possible to calculate an isochron-burial age for the LIM-IS2 samples as the $^{26}Al/^{10}Be$ values are higher than the surface ratio of 6.75. Given that no age can be determined from these samples, the results of this particular site are only discussed in the following paleo-erosion rates calculations.

Paleo-erosion rates

The in-situ ^{10}Be analytical data together with the inferred paleo-catchment-wide denudation rates obtained for the deposits are presented in Table 3. We have used the AMS-measured concentrations that were corrected for the production of the post depositional nuclide concentrations at sample depth *z* and atom loss due to radioactive decay since the deposition of the sediments (Table 3; since c. 500 ka). For the sample LIM-IS2, no ages could be calculated through isochron burial dating. However, considering that the sample is located stratigraphically in-between the sites LIM-PE3 and LIM-PE1, the depositional age of the sediments must also correspond to c. 500 ka. We thus used this age to correct the cosmogenic concentration for atom loss due to radioactive decay since the time of the deposition. Accordingly, this results in the following ^{10}Be concentrations at the time of deposition: 96492 ± 1927 atoms g^{-1} for LIM-PE1, 137436 ± 4894 atoms g^{-1} for LIM-PE2 and 155918 ± 6107 atoms g^{-1} for LIM-PE3. As a result of this, the calculated paleo-catchment wide denudation rates are 105 ± 10 mm ka^{-1} (LIM-PE3), 119 ± 11 mm ka^{-1} (LIM-PE2) and 169 ± 14 mm ka^{-1} (LIM-PE1) for the bottom, the middle and the top levels of the studied deposits, respectively (Table 3 and Figure 5).

Sediment provenance through U/Pb detrital zircon dating

For the Lima drainage basin, Litty et al. (2017) have shown that in-situ U/Pb zircon ages of modern sediments at the coast yield two distinct age populations (20 and 60 Ma; Figure 1 and 6). A modern sample farther upstream close to the inland limit of the costal batholith (Figure 1) yields a single main zircon-age population centred on ca. 20 Ma (Figure 6; Litty et al., 2017). The sample LIM-PE1 used in the analysis by Litty et al (2017) has been complemented to obtain a total of 107 dated grains (60 additional dated grains). Additionally, 44 and 70 zircon grains have been dated for sites LIM-PE2 and LIM-PE3 respectively (Figure 6). These samples record three zircon populations ranging between 8 and 16 Ma whereas sample LIM-PE1 shows only two populations in this age range. Age patterns of the three samples yield two large populations around 18 and 20 Ma and four

zircon populations ranging between 24 and 36 Ma. Then, the results of samples LIM-PE2 and LIM-PE1 return two populations around 44 Ma whereas the sample LIM-PE3 returns only one zircon population at 44 Ma. The main differences in-between the samples are observed in the zircon populations older than 44 Ma. The samples LIM-PE2 and LIM-PE3 chronicle a population around 64 Ma that is not observed in sample LIM-PE1. In addition, the sample LIM-PE3 exhibits indistinct age populations ranging between 72 and 80 Ma. Sample LIM-PE2 shows one zircon population at 68 Ma that is hidden in the 64 Ma cluster, and one population at c. 81 Ma. Results of the sample LIM-PE1 yield one population at 57 Ma that is not observed in the two other samples. Additionally, the sample records two populations at c. 68 and at c. 72 Ma. Finally, the three samples show one zircon population at c. 85 Ma.

DISCUSSION

The results of the isochron burial dating imply that the accumulation of the Lima Conglomerate occurred around 500 ka ago. The two sites (lowermost and topmost sites), separated by c. 30 m in the vertical section from each other, record identical ages within errors. These results imply that the sediment accumulated relatively fast and within a short time interval. This period of fast sediment accumulation was superseded by a phase of erosion and recycling of the previously deposited material through the combined effect of fluvial and wave activities, which resulted in the formation of the spectacular cliff at Lima. We have no age constraints to infer the time when the phase of sediment accumulation ended, and when waves and streams started to recycle and erode the conglomerates. Likewise, we lack age brackets to date the commencement of the conglomerate construction at Lima. In the following section, we discuss possible controls on the sediment accumulation of the Lima Conglomerate (uplift, eustatic sea level rise, climate-driven eroisional pulse) thereby considering the sedimentation ages, the recorded increase in denudation rates and the provenance signal.

Fan progradation and sediment accumulation in response to an erosional pulse

We interpret the construction of the Lima conglomerate as a response to a wave of erosion in the hinterland, thereby resulting in a sediment pulse, the progradation of the fan and the accumulation of coarse-grained material. In this context, the evidence for a 60% increase in ^{10}Be-based denudation rates becomes important.

The modern erosion rates that have been calculated in the lowermost reaches of the entire western Peruvian Andes (Reber et al., 2017) range from 9 mm ka^{-1} to 190 mm ka^{-1} with an average value of c. 38 mm ka^{-1}. The observed denudation rates increase either with mean basin slope angles or with mean annual water discharge suggesting a strong environmental control and no tectonic driving force on the denudation on a millennial time-scale. For the modern Rio Rimac, Reber et al. (2017) reported a basin-averaged denudation rate of c. 197,6 ± 43,3 mm ka^{-1}, which is higher than the rates calculated for the Lima Conglomerate deposits (104,6 ± 9,3 mm ka^{-1} to 169,6 ± 13,9 mm ka^{-1} from base to top). However, Rio Rimac sample is located farther upstream. Most important in this context, however, is the rapid 60% increase of the inferred paleo-wide denudation rates from 105 to 165 mm ka^{-1} within a very short timespan. We use this short-term increase to infer the occurrence of an erosional pulse in the hinterland, which most likely resulted in the accumulation and the progradation of the Lima Conglomerate alluvial fan. We thus consider that this inferred erosional pulse resulted in a relatively high sediment flux to the coast, causing the fan of the Rimac and Chillon Rivers to prograde and the Lima Conglomerates to accumulate. Once the hillslopes in the upstream catchment have been liberated from the regolith cover, sediment supply to the trunk stream decreased with the result that sediment flux in the trunk streams could have dropped below the transport capacity. This could have initiated the phase of erosion and recycling of previously deposited material. A similar scenario has been proposed for the construction of the terrace deposits in the Pisco valley about 200 km farther south (Steffen et al., 2009) where ages of the terrace deposits are 40 ka and 20 ka, and in the Pativilca valley 200 km farther north where multiple sets of conglomerate units yielded OSL ages of c. 20 and 100 ka (Trauerstein et al., 2014), and cosmo-based depth-profile ages of c. 200 ka and c. 1.2 Ma (Litty et al., 2018), albeit with large errors. Finally, ages of c. 20 ka, 40-60 ka and 100 ka have

also been reported for fan systems and terrace deposits in the Majes valley c. 650 km farther southeast. At Pisco, the accumulation and construction of valley fill conglomerates occurred during a period of fast erosion, as ^{10}Be-based paleo-denudation rates imply (Bekaddour et al., 2014). In the same sense, Norton et al. (2016) proposed that the deposition of fluvial conglomerates on valley floors was most likely associated with the occurrence of an erosional pulse on the bordering hillslopes, while the subsequent downcutting occurred as the sediment reservoirs on the bordering hillslopes became depleted. Following these lines, we propose that this inferred pulse of erosion could have been responsible for the relatively fast sediment aggradation and for the construction of the Lima Conglomerate.

The samples LIM-PE1, LIM-PE2 and LIM-PE3 show similarities in their zircon population and exhibit a more complex signal with a larger number of age populations compared to the modern river samples (Figure 6). The similarities observed between the three sand samples indicate that they share nearly identical sediments sources. The sediments were mainly eroded from the catchment of the Rio Rimac with some material supplied by the Rio Chillon. For example, the distinct peak at 20 Ma, which is found in the three samples, has been identified as representing zircon crystals derived from the upper part of the Rio Rimac catchment (Litty et al., 2017). The 72 Ma peak in the age pattern, which is also observed in the three samples, suggests that the material was most likely supplied from the coastal batholith in the Rio Chillon catchment (Mukasa et al., 1986). Additionally, the broader range of zircon ages in the three terrace samples indicates that the sediment of the matrix has been eroded from a broader area in comparison with the modern river sediments. Accordingly, these results are in line with those from our previous study (Litty et al., 2017). This implies that the modern sediment sources are mainly located along the steep middle reaches of the rivers, whereas during the period of the deposition of the alluvial fan material, sources were additionally located in the low-relief headwaters of these catchments (Litty et al., 2017). Note that the sample LIM-PE1 shows differences in its provenance compared to the two other samples (Figure 6). Because this shift in the erosional loci was coincident with higher erosion rates compared to the two other samples, we tentatively interpret that this change in the erosion rate might have affected the provenance signal.

Discarded possible controls on the inferred sediment pulses

A first explanation includes the scenario where a possible rainfall driven (or alternatively an earthquake triggered) landslide might have dammed a lake within the upstream valley. Breaching of this dam might have initiated a wave of sediment flux (Korup et al., 2010), thereby causing the alluvial fan to prograde and gravels to accumulate. Although this is a valuable interpretation, we do not favour this scenario because the recorded change in the cosmogenic signal requires an increase in erosion rates over an area that is much larger than the scale of individual or even multiple landslides and/or rock avalanches (e.g., von Blanckenburg, 2006). Indeed, landsliding, lake damming and breaching, and the resulting sediment pulse is unlikely to be recorded by a change in the concentrations of cosmogenic nuclides provided that these processes are widespread and occur over a broader time scale, as generic models of the dependency of ^{10}Be concentrations in stream sediments and landsliding in the upstream basin suggest (Niemi et al., 2005). The decrease in ^{10}Be concentration in the sediment sample and the inferred increase in basin-wide denudation rate during the accumulation of the Lima conglomerate thus suggest that changes in hillslope erosion and supply of sediment occurred over a large area. Indeed a localized sediment pulse on a hillslope would not be recorded by in situ cosmogenic ^{10}Be in stream sediments.

A second explanation includes the results of changes in uplift patterns. An uplift pulse could have initiated an increase of the erosion rates. However, we consider it unlikely that uplift has to be invoked to the explain the formation the Lima Conglomerate, because a compilation of stratigraphic and sedimentological data together with a geomorphological analysis of the coastal region of Peru has shown that the region between 6° and 14° latitudes has experienced a long-term phase of subsidence and not uplift (Viveen and Schlunegger, 2018). This sector also includes the region surrounding Lima.

As a third possibility, an eustatic sea level highstand could have lead to the accumulation of the Lima Conglomerate. Indeed, the c. 500 ka period corresponds to a relative sea level highstand. However, we discard the possibility that an eustatic sea level high stand could be the main factor controlling the pulse of sediment. While a sea-level rise, and also a highstand could be invoked to

explain the construction of an alluvial fan where streams debouch into the sea, such a mechanism is not capable of initiating an erosional pulse in the hinterland.

Possible climate controls on the inferred sediment pulses

Several climate-related mechanisms could be invoked to explain the inferred sediment pulses that are likely to be recorded by the provenance and ^{10}Be signals. In a first model, a shift towards higher precipitation rates has been interpreted as being the main factor controlling the formation of terrace deposits in the Peruvian Andes (Bekaddour et al., 2014; Litty et al., 2017). In a second model, it has been suggested that meltwater surges from the Andean Cordillera during interglacial stades could have caused the accumulation of coarse, reworked glacial moraine material in the Rimac and Chillon fans, thereby forming the Lima Conglomerate (Le Roux et al., 2000). Both models invoke a scenario where a change in the runoff together with a pulse of erosion in the upstream drainage basin resulted in the supply of large volumes of material, thereby controlling the formation of the Lima Conglomerate. The rapid increase in paleo-erosion rates during a short time span indicates that the sediment accumulation possibly corresponded to a pulse of erosion, which is compatible with the proposed two models outlined above. In addition, the contribution of large volumes of glaciogenic material is likely to result in a reduction of the ^{10}Be concentrations in stream sediments, as an analysis in an Alpine drainage basin has shown (Delunel et al., 2014). Moreover, the material of the Lima Conglomerate has been eroded from both the steep middle reaches and the low-relief headwaters (Altiplano) of the Rio Rimac (mainly) and Rio Chillon catchments, while the modern material is mainly derived from the lower steep reaches only (Litty et al., 2017). The provenance results, indicating that the Altiplano represents one of the main sediment sources, are also compatible with the two proposed models. Indeed, the first proposed model infers an increase in the precipitation rates on the Altiplano whereas the second model considers that the meltwater surged from the Andean Cordillera, thereby recycling glaciogenic material. These two mechanisms would lead to an increase of the erosion on the Altiplano and so to an increase of material fluxes with sources on the Altiplano. The paleo-erosion rates and provenance results thus do not allow distinguishing between the two proposed mechanisms.

We then use possible correlations between any known periods of enhanced precipitation or interglacial stades and the obtained accumulation ages to distinguish between the two models of sediment accumulation. The isochron burial age results suggest that the sediment accumulation has been relatively quick. Additionally, the results imply the occurrence of one period of aggradation only, which occurred around 500 ka ago. When considering the orbital and climatic parameters, the 500 ka-old period corresponds to a positive peak in the obliquity angle and to low precession parameters, and also to a time interval of inferred high radiative forcing due to high levels of CO_2 and CH_4, and to period when the relative temperature was considered to be high (Jouzel et al., 2007). We thus propose that the peaks in the precession parameters and the obliquity have exerted an orbital control on the sediment production. Indeed, on orbital time scales, larger heat contrasts were considered to have shifted the position of the ITCZ, thereby yielding stronger upper-air easterlies and more precipitation on the Altiplano, as recorded by lake level highstands on the plateau (Ouki, Minchin and Tauca pluvial periods, e.g., Baker et al., 2001a; Fritz et al., 2004). Additionally, the relative high inferred temperatures 500 ka ago are compatible with the model where the meltwater surges during interglacial stades caused a large supply of sediment and thus the formation of the Lima Conglomerate. This study suggests that both models could be invoked to explain the formation of the Lima Conglomerate, and both point towards an orbital control and interglacial meltwater surges on the erosion pulse and the sediment production.

We acknowledge, though, that the inferred interglacial period at 500 ka was rather weak (MIS 13.1), and that the subsequent even warmer interglacial starting at c. 440 ka (Jouzel et al., 2007) apparently lacks a corresponding sedimentary record. Indeed, we would expect that stronger interglacials should have a larger impact on the erosional history of a catchment and on a sedimentary record than a weaker one. It is possible that the Lima conglomerate is a composite of different units such as that the locus of deposition has shifted farther north during the subsequent warm period. We discard this interpretation because of the constant ages within the vertial section. Alternatively, it is also possible that warm and wet periods are associated with fluvial downcutting instead of sediment accumulation if the hillslope material was already depleated during a previous warm and erosive climate. Indeed, whether a warm, or wet period, is associated with an erosional and sedimentary pulse

crucially depends on the thickness of soils and hence the sediment reservoir on the hillslopes in a catchment, and on the magnitude-frequency distribution of precipitation during a particular warm period. Models show that the combination of both variables exerts a strong control on whether wet periods are associated with an erosional pulse and the accumulation of sediment on the valley floor, or with further fluvial dissection (Tucker and Slingerland, 1997; Norton et al., 2016). We lack the quantitative data to fully address these questions. However, MIS 13.1 was apparently preceded by a long period of continuous warming prior to peaking at 500 ka (except for a short colder time interval corresponding to MIS 13.2). The subsequent colder period between MIS 12.4 and 12.2 could have been too dry for the regolith to recover after the inferred erosional pulse during MIS 13.1 As a result, the even warmer period thereafter could have been characterized by thin soils, with the consequences that not enough material was available on the hillslopes to produce large volumes of material upon erosion. This is, of course, pure speculation, but it illustrates that whether warm periods may be recorded by terrace levels and conglomerate accumulation not only depends on a particular climate, but also on the preceding geologic and geomorphic history.

CONCLUSIONS: RELEVANCE OF THE LIMA CONGLOMERATE IN A BROADER CONTEXT

We suggest that the Lima Conglomerate, like other fluvial terrace systems in Peru (Trauerstein et al., 2014; Bekaddour et al., 2014. Norton et al., 2016), most likely formed in response to a possibly climate-driven sedimentary pulse, which was sustained enough in space to be recorded by changes in concentrations of cosmogenic ^{10}Be. As sediment flux then decreased, the river started to incise into the previously deposited conglomerates and started to recycle this material with support by the strong waves. Field work has shown that the coastline of Peru hosts many conglomerate fragments of unknown ages and provenance. We suggest that further dating of these archives would contribute to an improved understanding of how climate changes have imprinted on the erosional history of the Western Peruvian margin (Reber et al., 2017), mainly because a tectonic driving force particularly along the coastline can be ruled out as this area has been subsiding over geological time scales (Viveen and Schlunegger, 2018). We also suggest that the combination of (i) isochron burial dating of conglomerates with ^{10}Be and ^{26}Al, (ii) dating of detrital zircon minerals, and (iii) of estimations of

paleo-erosion rates using cosmogenic ^{10}Be will allow to quantitatively explore these archives for their ages, material provenance and process rates, which in turn is the basis for a better understanding of how erosion systems have possibly responded to climate and climate changes thereof. Our study thus illustrates the potential of these sedimentary archives for a better understanding of possible linkages between shifts in orbital parameters, and surface response including erosion and material transport (Strecker et al., 2007).

The inferred erosional pulse at Lima was likely to have occurred at the scale of nearly the entire drainage basin, supporting the idea of a large-scale, most likely climate driven control. In this context, the accumulation age of c. 500 ka falls into an orbital cycle (eccentricity). Climate changes, with orbital frequencies of c. 100 ka and multiples thereof, and of 40 ka and 20 ka were also considered to have controlled pulses of erosion, sediment discharge and the accumulation of material by modulating the fluvial runoff on the western Andean margin of Peru: Pativilca at 10°42'S (Trauerstein et al., 2014; Litty et al., 2018); the Pisco valley at 13°42'S (Steffen et al., 2009) and the Majes valley at 16°13'S latitudes (Steffen et al., 2010). Accordingly, the Andean mountain range could be perceived as an ideal laboratory for exploring a climate forcing on surface mass fluxes not only for the present-time, but also for the geologic history. Accordingly, while the erosional history in other regions on our planet might primarily record either tectonic (e.g., the Himalayas; Ouimet et al., 2009) or glacial signals (e.g., Schlunegger and Norton, 2013), the Peruvian Andes might serve as a better laboratory to investigate changes in precipitation possibly in response to an orbital forcing.

ACKNOWLEDGEMENTS

We thank Romain Delunel for his help in the calculation of the paleo denudation rates. This project has been funded by the Swiss National Science Foundation (project Number 137516).

REFERENCES

Akçar, N., Deline, P., Ivy-Ochs, S., Alfimov, V., Hajdas, I., Kubik, P. W., Christl, M., and Schlüchter, C ., 2012. The 1717 AD rock avalanche deposits in the upper Ferret Valley (Italy): A dating approach with cosmogenic 10Be. Journal of Quaternary Science, v. 27(4), p. 337–440.

Akçar, N., Ivy-Ochs, S., Alfimov, V., Schlunegger, F., Claude, A., Reber, R., Christl, M., Vockenhuber, C., and Schlüchter, C., 2017. Isochron-burial dating of glaciofluvial deposits: first results from the Swiss Alps. Earth Surface Processes and Landforms, v. 42(14), p. 2414-2425.

Andersen, T., 2005. Detrital zircons as tracers of sedimentary provenance: limiting conditions from statistics and numerical simulation. Chemical Geology, v.216, p. 249– 270.

Baker, P. A., Seltzer, G. O., Fritz, S. C., Dunbar, R. B., Grove, M. J., Tapia, P. M., Cross, S. L., Rowe, H. D., and Broda, J. P., 2001a. The history of South American tropical precipitation for the past 25,000 years. Science, v. 291, p. 640–643.

Balco, G., and Rovey, C. W., 2008, An isochron method for cosmogenic-nuclide dating of buried soils and sediments. American Journal of Science, v. 308(10), p. 1083-1114.

Balco, G., Stone, J. O., Lifton, N. A., and Dunai, T. J., 2008. A complete and easily accessible means of calculating surface exposure ages or erosion rates from Be-10 and Al-26 measurements. Quarternary Geochronology, v. 3, p. 174–195.

Balco, G., Soreghan, G. S., Sweet, D. E., Marra, K. R., and Bierman, P. R., 2013. Cosmogenic-nuclide burial ages for Pleistocene sedimentary fill in Unaweep Canyon, Colorado, USA. Quaternary Geochronology, v. 18, p. 149-157.

Bekaddour, T., Schlunegger, F., Vogel, H., Delunel, R., Norton, K. P., Akcar, N., and Kubik, P., 2014, Paleo erosion rates and climate shifts recorded by Quaternary cut-and-fill sequences in the Pisco valley, central Peru. Earth and Planetary Science Letters, v. 390, p. 103–115.

Bender A. M., Amos C. B., Bierman P., Rood D. H., Staisch L., Kelsey H., and Sherrod B., 2016. Differential uplift and incision of the Yakima River terraces, central Washington State. Journal of Geophysical Research, Solid Earth, v. 121, p. 365–384.

Bluck, B., 2010. Structure of gravel beaches and their relationship to tidal range. Sedimentology, v. 58, p. 994-1006.

Blum, M.D., and Törnqvist, T.E., 2000. Fluvial responses to climate and sea-level change: a review and look forward. Sedimentology, v. 47, p. 2-48.

Bookhagen, B., and Strecker, M.R., 2008, Orographic barriers, high-resolution TRMM rainfall, and relief variations along the eastern Andes. Geophysical Research Letters, v. 35, L06403, doi: 10 .1029 /2007GL032011.

Borchers, B., Marrero, S., Balco, G., Caffee, M., Goehring, B., Lifton, N., Nishiizumi, K., Phillips F., Schaefer, J., and Stone, J., 2016. Geological calibration of spallation production rates in the CRONUS-Earth project. Quaternary Geochronology, v. 31, p. 188-198.

Braucher, R., Merchel, S., Borgomano, J., and Bourles, D. L., 2011. Production of cosmogenic radionuclides at great depth: A multi element approach. Earth and Planetary Science Letters, v.

309(1), p. 1–9.Chmeleff, J., von Blanckenburg, F., Kossert, K., and Jakob, D., 2010. Determination of the Be-10 half-life by multicollector ICP-MS and liquid scintillation counting. Nuclear Instruments and Methods in Physics, Research Section B: Beam Interactions with Materials and Atoms, v. 268, p. 192-199.

Christl, M., Vockenhuber, C., Kubik, P. W., Wacker, L., Lachner, J., Alfimov, V., and Synal, H. A., 2013. The ETH Zurich AMS facilities: Performance parameters and reference materials. Nuclear Instruments and Methods in Physics Research Section B: Beam Interactions with Materials and Atoms, v. 294, p. 29-38.

Çiner A, Doğan U, Yıldırım C, Akçar N, Ivy-Ochs S, Alfimov V, Kubik PW, and Schlüchter C. 2015. Quaternary uplift rates of the Central Anatolian Plateau, Turkey: insights from cosmogenic isochron-burial nuclide dating of the Kizilirmak River terraces. Quaternary Science Reviews, v. 107, p.81-97.

Dadson, S. J., Hovius, N., Chen, H., Dade, W. B., Hsieh, M-L., Willett, S. D., Hu, J-C., Horng, M. J., Chen, M-C., Stark, C. P., Lague, D. and Lin, J. C., 2003. Links between erosion, runoff variability and seismicity in the Taiwan orogen. Nature, v. 426, p. 648-651.

D'Arcy, M., Whittaker, A. C., and Roda-Boluda, D. C., 2017. Measuring alluvial fan sensitivity to past climate changes using a self-similarity approach to grain-size fining, Death Valley, California. Sedimentology, v. 64(2), p. 388-424.

Darling, A. L., Karlstrom, K. E., Granger, D. E., Aslan, A., Kriby, E., Ouimet, W. B., and Cole, R. D., 2012. New incision rates along the Colorado River system based on cosmogenic burial dating of terraces: Implications for regional controls on Quaternary incision. Geosphere, v. 8(5), p. 1020-1041.

Delunel, R., Van der Beek, P. A., Bourlès, D. L., Carcaillet, J., and Schlunegger, F., 2014. Transient sediment supply in a high-altitude Alpine environment evidenced through a 10Be budget of the Etages catchment (French Western Alps). Earth surface processes and landforms, v. 39(7), p. 890-899.

Dodson, M., Compston, W., Williams, I., and Wilson, J., 1988, A search for ancient detrital zircons in Zimbabwean sediments: Journal of the Geological Society, v. 145, p. 977– 983.

Erlanger E. D., Granger D. E., and Gibbon R. J., 2012. Rock uplift rates in South Africa from isochron burial dating of fluvial and marine terraces. Geology, v. 40, p.1019-1022.

Fedo, C. M., Sircombe, K. N., and Rainbird, R. H., 2003. Detrital zircon analysis of the sedimentary record. Reviews in Mineralogy and Geochemistry, v. 53(1), p. 277-303.

Fritz, S. C., Baker, P. A., Lowenstein, T. K., Seltzer, G. O., Rigsby, C.A., Dwyer, G. S., and Luo, S., 2004, Hydrologic variation during the last 170,000 years in the southern hemisphere tropics of South America: Quaternary Research, v. 61, p. 95–104, doi: 10 .1016 /j .yqres .2003 .08 .007.

Garreaud, R., Vuille, M., and Clement, A. C., 2003. The climate of the Altiplano: Observed current conditions and mechanisms of past changes. Paleogeography, Paleoclimatology, Paleoecology, v. 194, p. 5–22.

Gosse, J. C., and Phillips, F. M., 2001. Terrestrial in situ cosmogenic nuclides: theory and application. Quaternary Science Reviews, v. 20(14), p. 1475-1560.

Granger, D. E., Kirchner, J. W., and Finkel, R. C., 1996. Spatially averaged long-term erosion rates measured from in situ-produced cosmogenic nuclides in alluvial sediment. Journal of Geology, v. 104, p. 249-257.

Granger D. E., 2006. A review of burial dating methods using 26Al and 10Be. Geological Society of America Special Publication, v. 415, p. 1-16.

Hansen, J., Sato, M., Russell, G., and Kharecha, P., 2013. Climate sensitivity, sea level and atmospheric carbon dioxide. Philosophical Transactions of the Royal Society A, v. 371, p. 20120294.

Jackson, S. E., Pearson, N. J., Griffin, W. L., and Belousova, E. A., 2004. The application of laser ablation-inductively coupled plasma-mass spectrometry to in situ U–Pb zircon geochronology. Chemical Geology, v. 211(1), p. 47-69.

Jouzel, J., Masson-Delmotte,V., Cattani, O., Dreyfus, G., Falourd, S., Hoffmann, G., Minster, B., Nouet, J., Barnola, J.M., Chappellaz, J., Fischer, H., Gallet, J.C., Johnsen, S., Leuenberger, M., Loulergue, L., Luethi, D., Oerter, H., Parrenin, F., Raisbeck, G., Raynaud, D., Schilt, A., Schwander, J., Selmo, E., Souchez, R., Spahni, R., Stauffer, B., Steffensen, J.P., Stenni, B., Stocker, T.F., Tison, J.L., Werner, M., and Wolff E.W., 2007. Orbital and Millennial Antarctic Climate Variability over the Past 800,000 Years. Science, v. 317, p. 793-796.

Karakouzian, M., Candia, M., Watkins, M.D., Wyman, R.V., and Hudyma, N., 1996. Geology of Lima, Peru. Geotechnical aspects. Boletin Sociedad Geologica del Peru, v. 85, p. 27-59.

Korup, O., Densmore, A.L., and Schlunegger, F., 2010, The role of landslides in mountain range evolution, Geomorphology, v. 120, p. 77-90.

Korschinek, G., Bergmaier, A., Faestermann, T., Gerstmann, U.C., Knie, K., Rugel, G., Wallner. A., Dillmann, I., Dollinger, G., Lierse von Gostomski, Ch., Kossert, K., Maiti, M., Poutivtsev, M., and Remmert, A., , 2010. A new value for the half-life of Be-10 by heavy-ion elastic recoil detection and liquid scintillation counting. Nuclear Instruments and Methods in Physics Research Section B: Beam Interactions with Materials and Atoms, v. 268, p. 187-191.

Kubik, P. W., and Christl, M., 2010. 10Be and 26Al measurements at the Zurich 6 MV Tandem AMS facility. Nuclear Instruments and Methods in Physics Research Section B: Beam Interactions with Materials and Atoms, v. 268(7-8), p. 880-883.

Kunz, B. E., Manzotti, P., von Niederhäusern, B., Engi, M., Darling, J. R., Giuntoli, F., and Lanari, P., 2017. Permian high-temperature metamorphism in the Western Alps (NW Italy). International Journal of Earth Sciences, v. 107(1), p. 203-229.

Lal, D., 1991. Cosmic ray labeling of erosion surfaces: in situ nuclide production rates and erosion models. Earth and Planetary Science Letters, v. 104 (2-4), p. 424-439.

Le Roux, J.P., Correa, C.T., and Alayza, F., 2000, Sedimentology of the Rímac- Chillón alluvial fan at Lima, Peru, as related to Plio-Pleistocene sea-level changes, glacial cycles and tectonics. Journal of South American Earth Sciences, v. 13, p. 499–510, doi: 10 .1016 /S0895 -9811 (00)00044 -4.

Lisson, C.I., 1907. Contribucion a la Geologica de Lima y sus Alrededores. Libreria e Imprenta Gil, Lima.

Litty, C., Lanari, P., Burn, M.,and Schlunegger, F., 2017. Climate-controlled shifts in sediment provenance inferred from detrital zircon ages, western Peruvian Andes. Geology, v. 45(1), p. 59-62.

Litty, C., Schlunegger, F., Akçar, N., Delunel, R., Christl, M., and Vockenhuber, C., 2018. Chronology of alluvial terrace sediment accumulation and incision in the Pativilca Valley, western Peruvian Andes. Geomorphology, v. 315, p. 45-56.

McPhillips, D., Bierman, P.R., and Rood, D. H., 2014, Millennial-scale record of landslides in the Andes consistent with earthquake trigger: Nature Geoscience, v. 7, p. 925–930, doi: 10 .1038 /ngeo2278.

Miall, A. D., 1985 Architectural element analysis: a new method of facies analysis applied to fluvial deposits. Earth- Science Reviews, v. 22, p. 261–308.

Montgomery, D. R., Balco, G., and Willett, S. D., 2001. Climate, tectonics, and the morphology of the Andes. Geology, v. 29, p. 579-582.

Morton, A. C., Claoué-Long, J. C., and Berge, C., 1996. SHRIMP constraints on sediment provenance and transport history in the Mesozoic Statfjord Formation, North Sea. Journal of the Geological Society, v. 153(6), p. 915-929.

Mukasa, S. B., 1986. Zircon U-Pb ages of super-units in the Coastal batholith, Peru: Implications for magmatic and tectonic processes. Geological Society of America Bulletin, v. 97, p. 241-254.

Niemi, N. A., Oskin, M., Burbank, D. W., Heimsath, A. M., and Gabet, E. J., 2005. Effects of bedrock landslides on cosmogenically determined erosion rates. Earth and Planetary Science Letters, v. 237, p. 480-498.

Norris, T. L., Gancarz, A. J., Rokop, D. J., and Thomas, K. W., 1983. Half-life of 26Al. Journal of Geophysical Research, Solid Earth, v. 88(S01).

Norton, K.P., Schlunegger, F., and Litty, C., 2016, On the potential for regolith control of fluvial terrace formation in semi-arid escarpments: Earth Surface Dynamics, v. 4, p. 147–157, doi: 10 .5194 /esurf -4 -147 -2016.

Ouimet, W. B., Whipple, K. X., and Granger, D. E., 2009. Beyond threshold hillslopes: Channel adjustment to base-level fall in tectonically active mountain ranges. Geology, v. 37(7), p. 579-582.

Paton, C., Woodhead, J. D., Hellstrom, J. C., Hergt, J. M., Greig, A., and Maas, R., 2010. Improved laser ablation U-Pb zircon geochronology through robust downhole fractionation correction. Geochemistry, Geophysics, Geosystems, v. 11(3). doi:10.1029/2009GC002618

Petrus, J. A., and Kamber, B. S., 2012. VizualAge: A novel approach to laser ablation ICP-MS U-Pb geochronology data reduction. Geostandards and Geoanalytical Research, v. 36(3), p. 247-270.

Reber, R., Delunel, R., Schlunegger, F., Litty, C., Madella, A., Akçar, N., and Christl, M., 2017. Environmental controls on 10Be-based catchment-averaged denudation rates along the western margin of the Peruvian Andes. Terra Nova, v. 29(5), p. 282-293.

Rohling E. J, Grant K, Bolshaw M, Roberts A. P, Siddall M, Hemleben C, and Kucera M., 2009. Antarctic temperature and global sea level closely coupled over the past five glacial cycles. Nature Geosciences, v. 2, p. 500–504.

Savi, S., Schildgen, T. F., Tofelde, S., Wittmann, H., Scherler, D., Mey, J., Alonzo, R. N., and Strecker, M. R., 2016. Climatic controls on debris-flow activity and sediment aggradation: The Del Medio fan, NW Argentina. Journal of Geophysical Research: Earth Surface, v. 121(12), p. 2424-2445.

Schaller, M., Ehlers, T. A., Stor, T., Torrent, J., Lobato, L., Christl, M., and Vockenhuber, C., 2016. Timing of European fluvial terrace formation and incision rates constrained by cosmogenic nuclide dating. Earth and Planetary Science Letters, v. 451, p. 221-231.

Schlunegger, F., and Norton, K. P., 2013. Water versus ice: The competing roles of modern climate and Pleistocene glacial erosion in the Central Alps of Switzerland. Tectonophysics, v. 602, p. 370-381.

Sláma, J., Košler, J., Condon, D. J., Crowley, J. L., Gerdes, A., Hanchar, J. M., and Schaltegger, U., 2008. Plešovice zircon—a new natural reference material for U–Pb and Hf isotopic microanalysis. Chemical Geology, v. 249(1), p. 1-35.

Steffen, D., Schlunegger, F., and Preusser, F., 2009. Drainage basin response to climate change in the Pisco valley, Peru. Geology, v. 37, p. 491-494, doi: org/10.1130/G25475A.1.

Steffen, D., Schlunegger, F., and Preusser, F., 2010. Late Pleistocene fans and terraces in the Majes valley, southern Peru, and their relation to climate variations. International Journal and Earth Sciences, v. 99, p. 1975-1989, doi: 10.1007/s00531-009-0489-2.

Stone, J. O., 2000. Air pressure and cosmogenic isotope production. Journal of Geophysical Research v. 105(B10), p. 23753-23759

Strecker, M. R., Alonso, R. N., Bookhagen, B., Carrapa, B., Hilley, G. E., Sobel, E. R., and Trauth, M. H., 2007, Tectonics and climate of the southern central Andes. Annual Review of Earth and Planetary Sciences, v. 35, p. 747–787, doi: 10 .1146 /annurev .earth .35 .031306 .140158.

Sylvia, D. A., and Galloway, W. E., 2006. Morphology and stratigraphy of the late Quaternary lower Brazos valley: Implications for paleo-climate, discharge and sediment delivery. Sedimentary Geology, v. 190(1), p. 159-175.

Tofelde, S., Schildgen, T. F., Savi, S., Pingel, H., Wickert, A. D., Bookhagen, B., Wittmann, H., Alonso, R. N., Cottle, J., Strecker, M. R., 2017. 100 kyr fluvial cut-and-fill terrace cycles since the Middle Pleistocene in the southern Central Andes, NW Argentina. Earth and Planetary Science Letters, v. 473, p. 141-153.

Trauerstein, M., Norton, K. P., Preusser, F., and Schlunegger, F., 2013. Climatic imprint on landscape morphology in the western escarpment of the Andes. Geomorphology, v. 194, p. 76-83.

Trauerstein, M., Lowick, S. E., Preusser, F., and Schlunegger, F., 2014, Small aliquot and single grain IRSL and post-IR IRSL dating of fluvial and alluvial sediments from the Pativilca valley, Peru. Quaternary Geochronology, v. 22, p. 163-174, doi: org/10.1016/j.quageo.2013.12.004.

Tucker, G. E., and Slingerland, R., 1997. Drainage basin responses to climate change. Water Resources Research, v. 33(8), p. 2031-2047.

Veit, H., May, J. H., Madella, A., Delunel, R., Schlunegger, F., Szidat, S., and Capriles, J. M., 2016. Palaeo- geoecological significance of Pleistocene trees in the Lluta Valley, Atacama Desert. Journal of Quaternary Science, v. 31(3), p. 203-213.

Vermeesch, P., 2004. How many grains are needed for a provenance study? Earth and Planetary Science Letters, v. 224(3), p. 441-451.

Viveen, W., and Schlunegger, F., 2018. Prolonged extension and subsidence of the Peruvian forearc during the Cenzoic. Tectonophysics, v. 730, p. 48-62.

Von Blanckenburg F. 2005. The control mechanisms of erosion and weathering at basin scale from cosmogenic nuclides in river sediment. Earth and Planetary Science Letters, v. 237(3), p. 462–479.

Wilson, P. A., 1975. K-Ar age studies in Peru with special reference to the emplacement of the Coastal batholith. Unpublished PhD thesis, University of Liverpool, Liverpool, England.

Table 1: *Sample locations and information about the samples used in this paper.*

Sample name		Latitude (°DD)	Longitude (°DD)	Altitude (m)	Isochron/ paleo erosion rates/ provenance	Material used
LIM-IS1	LIM-IS1-1 LIM-IS1-2 LIM-IS1-4 LIM-IS1-8	12.12103S	77.04414W	51	Isochron burial dating	Quartz rich pebbles
LIM-PE1					Paleo-erosion rate	Quartz in the sand
LIM-PE1					Provenance	Zircon in the sand
LIM-IS2	LIM-IS2-3 LIM-IS2-7 LIM-IS2-9 LIM-IS2-2 LIM-IS2-4 LIM-IS2-6	12.12141S	77,04443	42	Isochron burial dating	Quartz rich pebbles
LIM-PE2					Paleo-erosion rate	Quartz in the sand
LIM-PE2					Provenance	Zircon in the sand
LIM-IS3	LIM-IS3-2 LIM-IS3-4 LIM-IS3-5	12.12166S	77.04443W	18	Isochron burial dating	Quartz rich pebbles
LIM-PE3					Paleo-erosion rate	Quartz in the sand
LIM-PE3					Provenance	Zircon in the sand

Table 2: *Results of the AMS measurements $^{10}Be/^{9}Be$ and $^{26}Al/^{27}Al$ ratios (with uncertainties) as well as calculated ^{10}Be, ^{26}Al concentrations and $^{26}Al/^{10}Be$ ratio for each sample.*

	Sample name	Quartz dissolved (g)	9Be spike(mg)	10Be/9Be	Relative uncertainty(%)	Nb of 10Be in Sample per g	10Be Error in Conc	Total Al (mg)	26Al/27Al	Relative uncertainty (%)	Nb of 26Al in Sample per g	26Al Error in Conc	26Al/10Be
LIM-IS1	LIM-IS1-1	50,3701	0,1738	7,410E-13	3,47	170298,580	5934,5545	3,894	4,32E-13	40,9	744681,555	304303,654	4.37 ± 1.79
	LIM-IS1-2	40,0405	0,1973	1,845E-13	4,70	59965,986	2855,1116	3,903	1,78E-13	3,7	386955,219	14461,840	6.45 ± 0.39
	LIM-IS1-4	40,0253	0,1984	4,484E-14	7,60	14052,358	1129,9221	4,369	3,37E-14	12,7	81980,642	10403,450	5.83 ± 0.88
	LIM-IS1-8	40,6618	0,1992	6,741E-14	9,05	21275,286	1996,7165	5,317	4,92E-14	10,1	143496,429	14452,234	6.74 ± 0.93
LIM-IS2	LIM-IS2-3	50,6711	0,173	9,148E-14	9,05	20318,336	1889,0108	5,2026	1,017E-13	27,1	233067,794	63141,000	11.47 ± 3.29
	LIM-IS2-7	47,5302	0,1741	5,046E-14	9,94	11757,894	1228,5979	4,4252	1,790E-13	21,9	371951,678	81301,363	31.63 ± 7.66
	LIM-IS2-9	50,285	0,1734	1,649E-13	4,78	37449,245	1815,6724	5,6846	4,970E-13	35,5	1253894,222	445525,180	33.48 ±12.01
	LIM-IS2-2	39,4746	0,2002	8,000E-14	7,99	26291,647	2166,3029	4,5664	8,239E-14	6,8	212709,460	14551,774	8.09 ± 0.87
	LIM-IS2-4	26,1164	0,1973	3,778E-14	7,54	17850,770	1439,5593	2,4700	6,870E-14	5,3	145022,963	7641,243	8.12 ± 0.78
	LIM-IS2-6	40,0764	0,2002	3,238E-14	9,05	10000,943	979,3893	7,7009	3,155E-14	8,7	135328,504	11757,055	13.53 ± 1.77
LIM-IS3	LIM-IS3-2	33,054	0,1747	3,4617E-13	3,49	121401,824	4261,7543	3,4385	2,99E-13	2,7	693137,9828	18909,819	5.71 ± 0.19
	LIM-IS3-4	30,916	0,1698	5,6119E-14	6,51	19708,319	1342,0266	2,1612	1,01E-13	4,4	157330,2721	6977,656	7.98 ± 0.52
	LIM-IS3-5	35,149	0,1748	4,1767E-14	10,43	13076,147	1447,9297	2,7533	6,12E-14	5,3	106969,5149	5690,629	8.18 ± 0.85

Table 3: *In-situ ^{10}Be analytical data together with the inferred paleo-catchment-wide denudation rates obtained for the alluvial sediment.*

Sample name	Paleo/modern erosion rates	Age of the deposits	Quartz dissolved (g)	9Be spike(mg)	10Be/9Be	Relative uncertainty(%)	10Be concentration (at/g)	Concentration at the time of deposition (at/g)	Denudation rates (mm/ka)
LIM-ME*	Modern erosion rates	Modern river	50,1962	0,1994	3,96213E-13	12,0029	104528.69 +/- 12623.57	idem	197,6 +/- 43,3
LIM-PE1	Paleo erosion rates	Terrace	35,4465	0,1984	2,45031E-13	5,641	90738.85 +/- 541.32	96492 +/- 1927	169,6 +/- 13,9
LIM-PE2	Paleo erosion rates	Terrace	24,9508	0,1994	2,16661E-13	5,082	114408.53 +/- 665.85	137436 +/-4894	118,8 +/- 10,4
LIM-PE3	Paleo erosion rates	Terrace	37,7754	0,199	3,52575E-13	4,784	123258.61 +/- 589.66	155918 +/- 6107	104,6 +/- 9,3

*Reber et al., 2017

the error takes into account the error on the 10Be measurement + error on the age

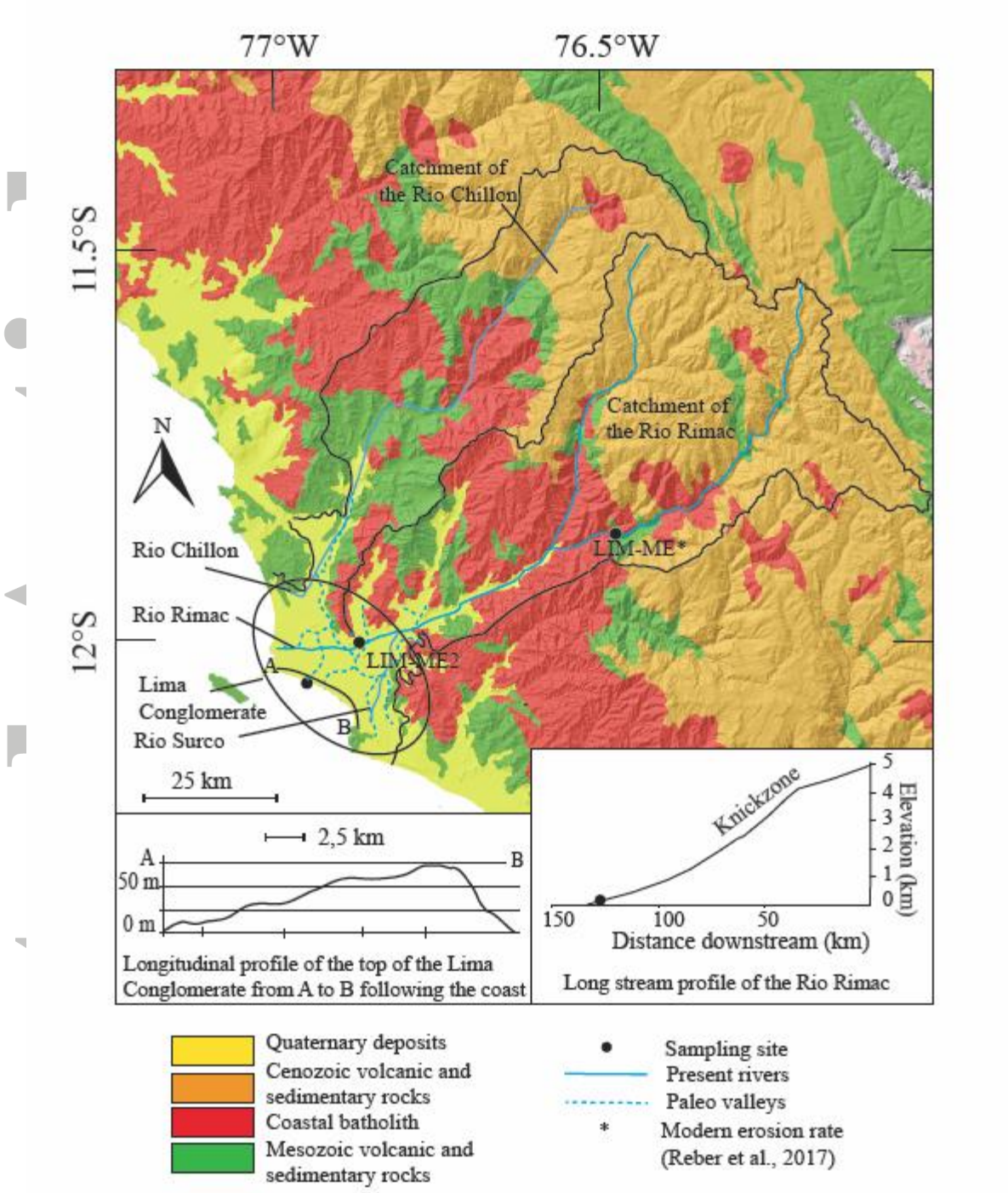

Figure 1: *Geological map of the study area showing the Lima Conglomerate and the catchments of the Rio Chillon and Rio Rimac.*

Figure 2: *A. and B. Photographs of the Lima Conglomerate at Miraflores. C. Sampling site for the isochron burial dating (LIM-IS1); the paleo-erosion rate and the sediment provenance (LIM-PE1) for the top level of the studied sequence. D. Close-up of the deposits of the topmost level. E. Sampling site for the isochron burial dating (LIM-IS2); the paleo-erosion rate and the sediment provenance (LIM-PE2) for the middle level of the sequence. F. Close-up of the deposits of the LIM-IS2 site (middle level). G. Sampling site for the isochron burial dating (LIM-IS3); the paleo-erosion rate and the sediment provenance (LIM-PE3) for the top level of the sequence. H. Close-up of the deposits of the lowermost level. The ellipses represent the sampling locations.*

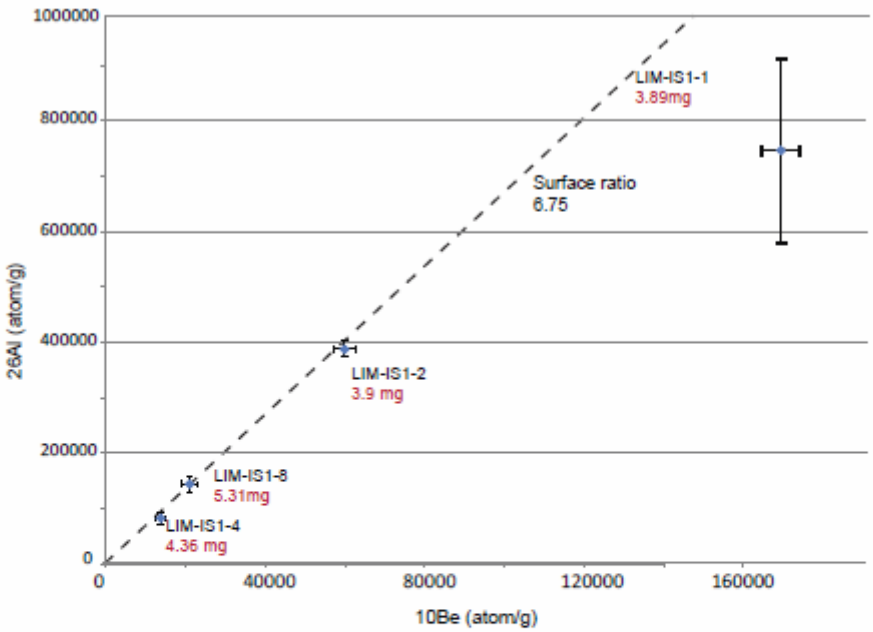

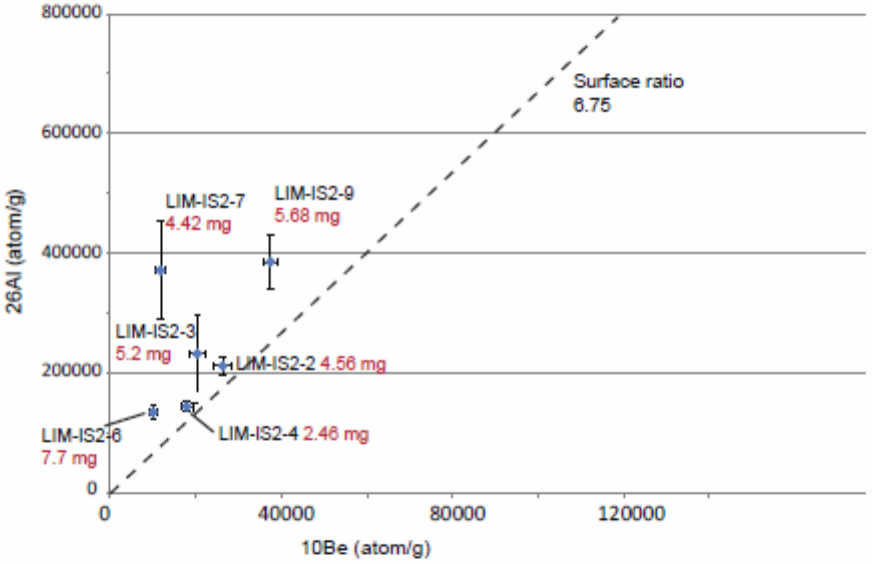

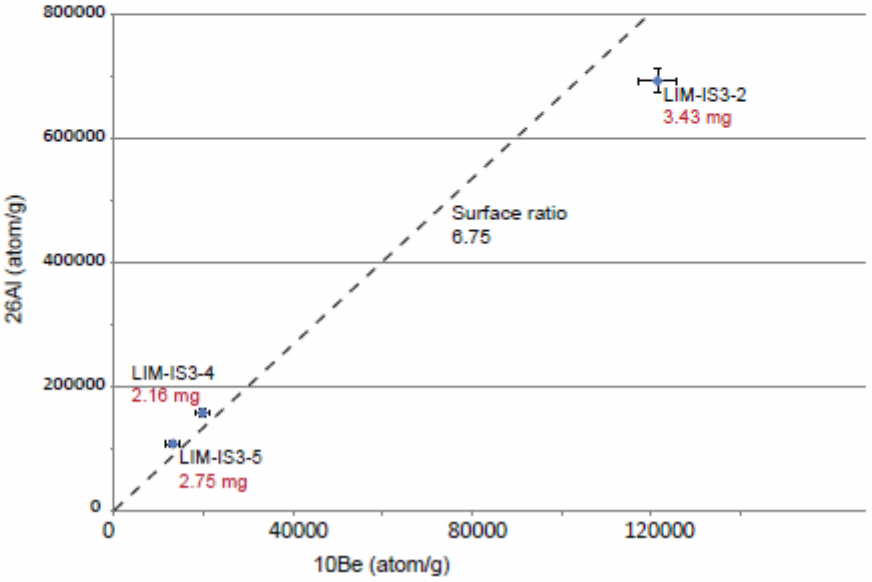

Figure 3: *Measured 26Al concentrations plotted versus 10Be concentrations of the samples designed for isochron burial dating LIM-IS1, LIM-IS2 and LIM-IS3 techniques. The error represents 1σ uncertainties. The dashed lines illustrate the surface rate ratio of 6.75 (Balco et al., 2008; Akçar et al., 2017).*

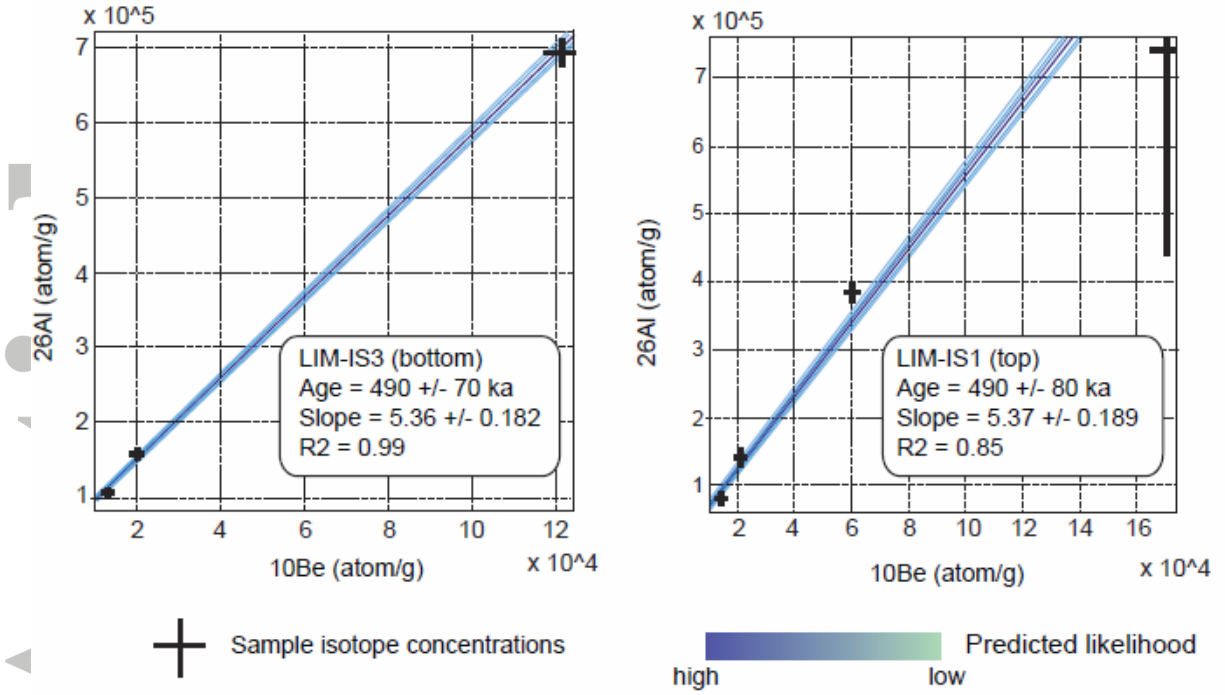

Figure 4: *Cosmogenic ^{26}Al-^{10}Be isochron plots for samples collected at the topmost and lowermost sites, constructed using a Bayesian linear regression algorithm modelling the likelihood of 100,000 lines fit to the isotope data. Crosses represent 1σ uncertainties from isochron analysis.*

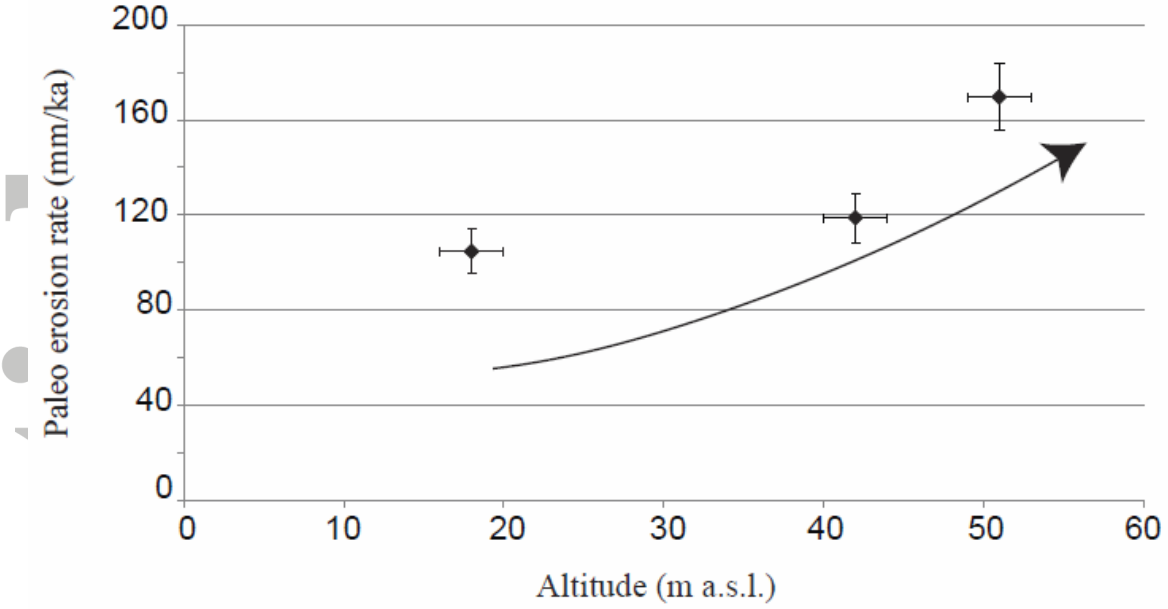

Figure 5: *Erosion rate during the time of sediment accumulation versus the altitude of the sampling site. This shows an increase of the paleo erosion rate with the altitude.*

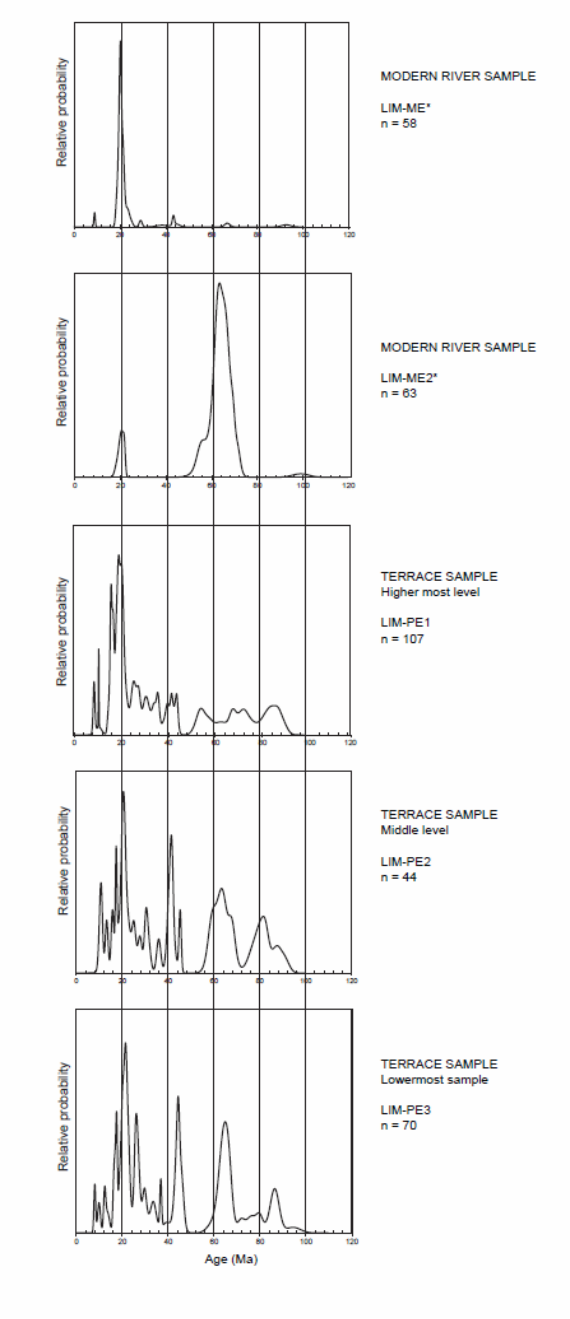

Figure 6: *Density probability diagrams of the detrital zircon U-Pb ages. *Complementary data from Litty et al., 2017.*